Publishing Excellence Inspiring Progress
ARISTON PUBLICATIONS
MatSci Express
ISSN: 2997-8440 www.aristonpubs.com/matsci-express https://doi.org/10.69626/mse.2024.0116

RESEARCH ARTICLE

Magnetic Nanoparticles in Cancer Thermotherapy: A Mathematical Approach to Optimal Treatment Design

F. A. Zargar [1, *], Hilal A. Bhat [2], Mohd. A. Zargar [3, *], S. A. Malik [4]

ABSTRACT: Thermotherapy, often called Hyperthermia treatment is a cancer treatment modality that involves raising the temperature of the tumor mass to over 315 K (42°C) for a specific duration, which leads to cell death through apoptosis or necrosis. Magnetic Particle Hyperthermia (MPH) is a non-invasive technique where magnetic nanoparticles are introduced into the tumor and then exposed to a magnetic field which convert magnetic energy into heat. Due to their high acidity, tumor cells are more sensitive to heat than healthy cells, meaning that heating the tumor to 315-319 K (42°C–46°C) can destroy it with minimal damage to the surrounding healthy tissues. During hyperthermia treatment, blood perfusion helps protect the healthy tissues around the tumor by dissipating excess heat. This paper presents a study where the temperature profiles within a spherical hepatic tumor mass are estimated by solving Pennes' Bio-heat Equation, incorporating a power term. The study uses analytical methods to examine the effects of magnetic fluid hyperthermia treatment. Numerical illustrations are carried out using magnetite (Fe_3O_4) nanoparticles having an average diameter of 10.9 nm with mineral oil as a carrier liquid, subjected to magnetic fields of varying intensities. By analysing the model, the present work helps in designing an optimal treatment protocol by identify the time threshold of the therapy for varying magnetic field strengths.

Keywords: Thermotherapy, Magnetic Fluid Hyperthermia, cancer treatment, Pennes' Bioheat Equation.

Received: 23 January 2024; Revised: 17 March 2024; Accepted: 15 April 2024; Published Online: 01 June 2024

1. INTRODUCTION

Cancer is primarily a genetic disorder, although environmental and other non-genetic factors also play significant roles in its development [1]. It is widely acknowledged that cancer arises from mutations in certain genes that make individuals more susceptible to the disease [2]. These genes are classified into three groups: gatekeepers, caretakers, and landscapers. Gatekeeper genes directly control cell growth and differentiation and include both oncogenes and tumor-suppressor genes (TSGs) [3]. Caretaker genes, on the other hand, indirectly promote tumorigenesis by preserving genomic integrity. When caretaker genes mutate, they can lead to genetic instability, resulting in the rapid accumulation of additional mutations in genes that directly regulate cell birth and death [4]. Landscaper genes, while not directly affecting cell growth, create an abnormal tissue environment that supports the transformation of cells into cancerous ones [5]. However, a single gene mutation is not enough to cause full-blown cancer. Further genetic mutations are needed for the disease to progress to malignancy and invasion. Thus, the risk of developing cancer depends not only on the initial mutations that start tumorigenesis but also on subsequent mutations that drive tumor progression [6, 7]. Cancer treatment modalities encompass a range of approaches, each specific to, type, stage, and characteristics of the cancer. Major treatment methods include surgery, chemotherapy, thermotherapy, and

[1] Govt Medical College, Bakshi Nagar, Jammu – 180001, India
[2] Department of Electronics & Instrumentation Technology, University of Kashmir, Srinagar – 190006, India
[3] Department of Computer Science, University of Saskatchewan, Saskatoon – S7N 5A2, Canada
[4] Higher Education Department, Government of Jammu & Kashmir – 190001, India

* Author to whom correspondence should be addressed:
faizanzgr@gmail.com (F.A. Zargar)
mohammad.zargar@usask.ca (Mohd. A. Zargar)

radiation therapy.

Hyperthermia is a condition in which tissue temperature is elevated to unusually high levels. In medical applications, it has been adapted to treat various cancers, offering the advantage of being non-invasive compared to surgical ablation and proving particularly useful for treating inoperable areas of the body [8, 9]. Magnetic fluids generate heat when placed in a magnetic field by converting magnetic field energy into thermal energy. The intensity of the generated heat depends on various parameters related to the magnetic field, such as frequency and amplitude, as well as the composition of the magnetic fluid, including particle size distribution, particle type, carrier liquid, and surface-active agents. The behavior of magnetic fluids in magnetic fields has been extensively studied, leading to their application in medical science, though development is ongoing to optimize heating of target tissues while minimizing damage to surrounding healthy tissues [4].

Advancements in the field of nanomaterial science have led to the opening of new horizons in nano-medicine [10-23]. In 1999, Lacis [13] attempted to study fluid movement at specific frequencies of applied magnetic fields. Mody et al. [15] reviewed how the magnetic properties of nanoparticles depend on their shape, size, surface coating, and doping, and discussed the clinical status of magnetic nanoparticles for magnetic fluid hyperthermia applications. Earlier Zakinyan et al. [22] had investigated the behavior of a drop of kerosene-based magnetic fluid composed of 10 nm magnetite nanoparticles surrounded by a nonmagnetic liquid on a solid horizontal surface under a low-frequency (≃1 Hz) uniform Rotating Magnetic Field (RMF). Dieckhoff et al. [8] used phase-lag research to study the behavior of magnetic nanoparticles exposed to RMF and Alternating Magnetic Field (AMF) at low frequencies. The dynamic behavior of particles in a magnetic field was also explained by solutions to the Fokker–Planck equations [21]. Beković et al. [3] proposed a new measuring system for characterizing magnetic flux losses and generated a high-frequency RMF with adequate amplitudes, making hyperthermia more applicable in medical science. Kumar et al. [4] explored the formulations of superparamagnetic iron oxide, gold nanorods and nanoshells, and carbon nanotubes for magnetic nanoparticle hyperthermia. Darvishi et al. [6] developed a method to analyze drug delivery and the distribution of magnetic nanoparticles in fluid hyperthermia cancer treatment, demonstrating the impact of nanoparticle distribution on treatment effectiveness. Recently in 2022, Ahmed et al. [1] studied the magnetic locomotion of Superparamagnetic iron oxide nanoparticles (SPIONs) under with RMF while controlling heating using AMF, demonstrating the feasibility of using SPIONs for targeted hyperthermia therapy.

Magnetic fluid hyperthermia works by generating heat through the energy loss of magnetic nanoparticles inside an Alternating Magnetic Field (AMF) or a Rotating Magnetic Field (RMF). This heat is sufficient to damage cancer cells, leading to their destruction through necrosis and apoptosis, effectively targeting the tumor. Necrosis occurs when cells are exposed to extreme conditions that deviate significantly from their normal environment, causing irreversible damage to their internal structures.

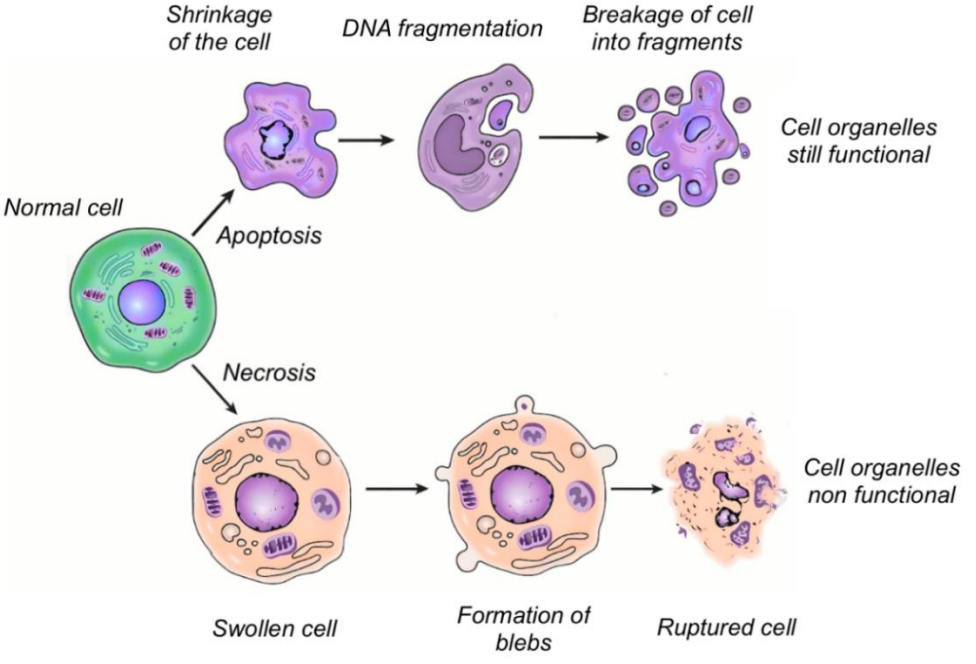

Fig. 1. Cell death mechanisms.

This process leads to rapid cell and tissue death and is characterized by being passive and un-programmed. Apoptosis, on the other hand, is a form of programmed cell death (PCD) that plays a crucial role in regulating and controlling an organism's growth and development. Often referred to as cellular suicide, apoptosis involves the cell actively participating in its own death. The process includes the cell shrinking, condensing, and ultimately fragmenting, ensuring a controlled and orderly elimination of damaged or unnecessary cells [19]. Both the mechanisms are depicted diagrammatically in Fig. 1.

Magnetic nanoparticles are administered directly to the tumor site through injection. Once in place, an alternating or rotating magnetic field is applied, causing the nanoparticles to generate heat through energy conversion mechanisms such as hysteresis loss and Néel or Brownian relaxation. This heat is then transferred to the surrounding tumor tissue, raising its temperature, and leading to cell death [19]. In this study, we propose a novel therapeutic control model for cancer treatment that studies the temperature profiles within a tumor mass during thermotherapy treatment using magnetic nanofluids. The significance of this research lies in integrating the fields of material science and mathematics with medicine to design a proper treatment modality. The section 3 of this paper outlines our proposed model in the form of a second order partial differential equation, the Pennes' bio-heat equation with appropriate boundary conditions modified to incorporate the heating effect from magnetic nanofluids under the influence of a magnetic field. In Section 4, we present numerical simulations to demonstrate the validity of the results. Finally, we discuss our findings and outline some potential avenues for future research.

2. MATHEMATICAL COMPUTATIONAL DETAILS

For the sake of this study, magnetic nanofluid consisting of Magnetite (Fe_3O_4) nanoparticles having a mean diameter of 10.9 nm with mineral oil as a carrier liquid is used on a Chinese hamster with primary hepatic tumor for thermotherapy. Magnetic nanofluid is directly injected at the tumor site and is assumed to be normally distributed within the tumor mass from its center up to radial extent r_0. Alternating magnetic field and Rotating magnetic field of varying intensities is generated using the supply coil assembly illustrated in Fig. 2 [3, 20]. Temperature profiles inside the tumor mass of size 2 cm are modelled by approximating the tumor mass as a sphere of radius (R) (see Fig. 3).

3. RESULTS AND DISCUSSION

3.1. Theory of power dissipation

Magnetic relaxation is a measure of the tendency of a magnetic system to maintain equilibrium or a steady-state condition upon a change in the magnetic field. The characteristic times that are required to reach this equilibrium are known as relaxation times.

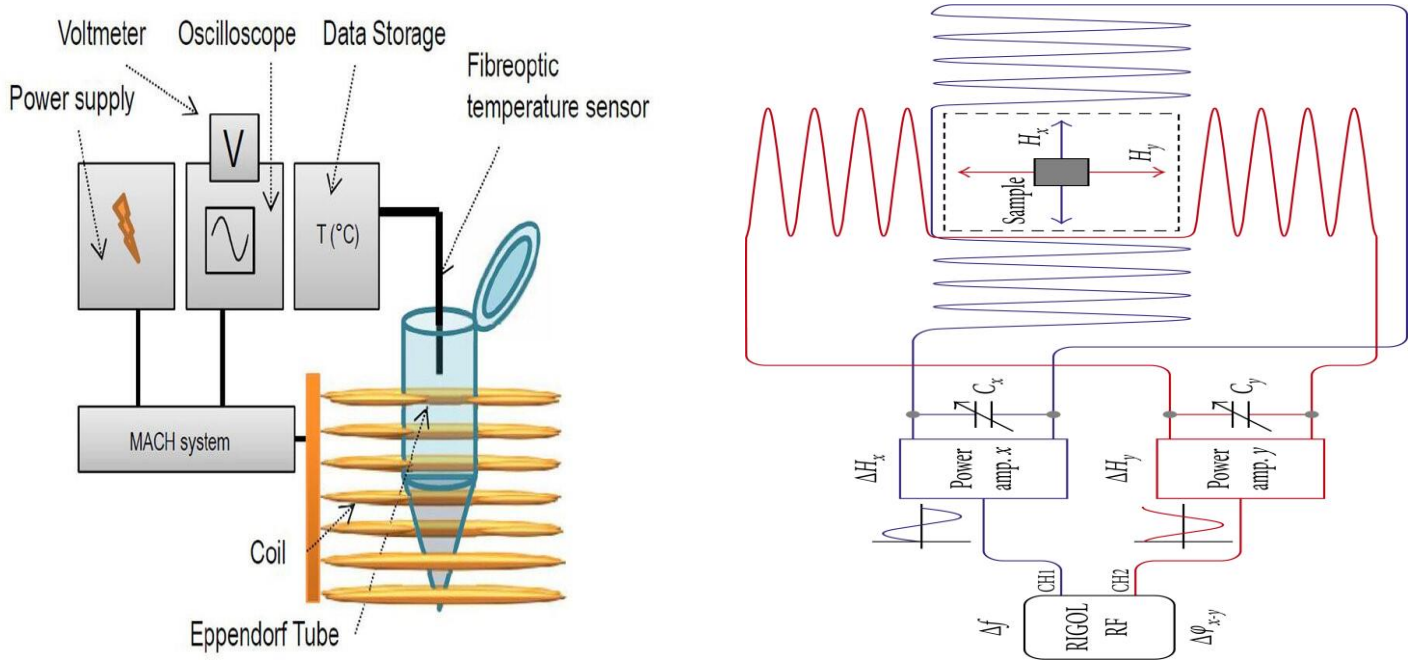

Fig. 2. Schematic representation of experimental setup for generating AMF (left) and RMF (right).

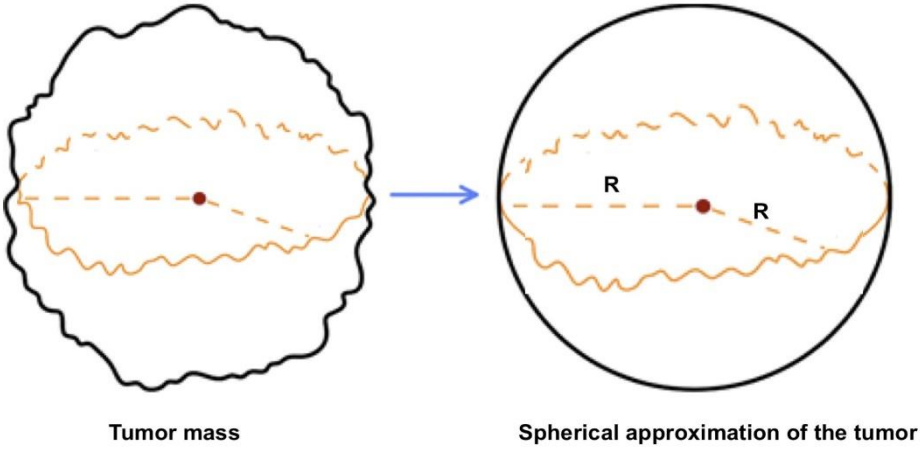

Fig. 3. Spherical approximation of the tumor mass

Magnetic relaxation of a single domain magnetic nanoparticle suspended in a fluid can be explained by Brownian Relaxation and Néel Relaxation theories Néel relaxation is caused by magnetization vector reorientation against an energy barrier inside the nanoparticle magnetic core while Brownian relaxation is a result of rotational diffusion of the magnetic nanoparticle as a whole in the carrier liquid [18]. The Néel and Brownian relaxation times, τ_N and τ_B [11] are respectively given as:

$$\tau_N = \tau_0 \exp\left(\frac{K_U V_M}{k_b T}\right) \tag{1}$$

$$\tau_B = \frac{3\eta V_H}{k_b T} \tag{2}$$

where τ_0, K_U, V_M, k_b, T, η, and $V_H = \left(\frac{1+2\delta}{D}\right)^3 V_M$ are the characteristic time constant (=10^{-9}), anisotropy constant, primary volume of the MNPs, Boltzmann constant, temperature, viscosity of the solvent, and hydrodynamic volume of the MNPs, respectively and δ is the thickness (= 10^{-9} m) of sorbed layer of the surfactant.

Rosensweig [18] proposed that Néel and Brownian relaxations happen simultaneously, with the effective relaxation angular frequency being the inverse of the effective relaxation time, as expressed by

$$\omega_{eff} = \frac{1}{\tau} = \frac{1}{\tau_N} + \frac{1}{\tau_B} \tag{3}$$

For sufficiently strong magnetic fields, the Néel relaxation time can vary significantly, changing by several orders of magnitude, while the Brownian relaxation time remains largely unaffected by the magnetic field strength. Consequently, the Néel relaxation mechanism becomes crucial. Beković et al. [3] gave a modified expression for power dissipation that incorporates thermal relaxation within the confines of linear response theory, given by:

$$P_0 = \mu_0 \pi \chi_0 f H_0^2 \frac{2\pi f\tau}{1+(2\pi f\tau)^2} \tag{4}$$

where μ_0 denotes the magnetic permeability of the free space, χ_0 – the equilibrium susceptibility, f and H_0 – the frequency and the amplitude of Alternating Magnetic Field (AMF), $\chi_0 = \chi_i \frac{3}{\zeta}\left(\coth\zeta - \frac{1}{\zeta}\right)$ where $\chi_i = \frac{\mu_0 \phi M_d^2 V_M}{3k_B T}$ and $\zeta = \frac{\mu_0 M_d H V_M}{k_B T}$, $H = H_0 \cos(2\pi f t)$, M_d is the domain magnetization of a suspended particle, and $V_M = \frac{\pi}{6} D^3$.

Power Loss P_0 in the RMF is determined by the fluid's physical properties and the parameters of the rotating magnetic field, as described in [3]. This relationship is expressed by the following equation.

$$P_0 = \mu_0 \frac{\Omega}{2}\left(m_x H_x + m_y H_y\right) \tag{5}$$

where H_x and H_y represent magnetic field strengths along $x-direction$ and $y-direction$ respectively, $\Omega = 2\pi f$ is the angular frequency, m_x and m_y are the resolved magnetization components of the magnetic field along x-direction and y-direction respectively. As the tissue temperature rises, the body's thermoregulation system

dissipates the excess heat by increasing blood flow to the tumor area. In response to this temperature increase, the blood flow rate in the surrounding healthy tissues multiplies significantly, whereas within the tumor itself, the blood flow rate only doubles at most. This mechanism helps protect the healthy tissues to a certain extent [10].

3.2. Governing Equation

The fundamental equation to describe heat transfer in biological tissues was proposed by H.H. Pennes [16]. This equation takes into account both heat conduction within tissues and heat transfer by blood perfusion. It is a partial differential equation that has been foundational in the field of thermal therapy and bioheat transfer modeling. The equation is given by,

$$\rho_p c_p \frac{\partial T}{\partial t} = \nabla \cdot (k \nabla T) + \rho_b c_b \omega_b (T_a - T) + Q \qquad (6)$$

where ρ_p and c_p are the density and specific heat capacity of the tumor mass, k is the thermal conductivity, ρ_b and c_b the density and specific heat capacity of blood, ω_b the blood perfusion rate, T_a the arterial blood temperature, Q the constant heat generation due to metabolism.

The modified radial form, which incorporates a power term P from a heating source, is expressed as,

$$\rho_p c_p \frac{\partial T}{\partial t} = k\left[\frac{1}{r^2}\frac{\partial}{\partial r}\left(r^2 \frac{\partial T}{\partial r}\right)\right] + \rho_b c_b \omega_b (T_a - T) + Q + P \qquad (7)$$

Assuming our domain is a spherical tumor mass with a radius R and that the applied heat does not affect the surrounding region, the equation is subject to the following conditions.

Initial Condition:

The temperature at $t = 0$ is assumed to be the same as core body temperature or the arterial blood temperature T_a.

Boundary Conditions:

$k\frac{\partial T}{\partial r} = 0$, when $r = 0$ and $r = R$.

3.2.1. Solution of the model

Substituting $\Phi = T_a - T$, equation (7) can be written as:

$$\rho_p c_p \frac{\partial \Phi}{\partial t} = k\left[\frac{1}{r^2}\frac{\partial}{\partial r}\left(r^2 \frac{\partial \Phi}{\partial r}\right)\right] + (\rho_b c_b \omega_b)\Phi + Q + P \qquad (8)$$

Using $\Phi = \frac{\varphi}{r}$, the above equation reduces to

$$\frac{\rho_p c_p}{k}\frac{\partial \varphi}{\partial t} = \left[\frac{\partial^2 \varphi}{\partial r^2}\right] + (\rho_b c_b \omega_b)\frac{\varphi}{k} + \frac{r}{k}(Q + P) \qquad (9)$$

In order to solve the above equation, we apply the Fourier sine transform throughout. Thus, we have

$$\sqrt{\frac{2}{\pi}}\int_0^\infty \frac{\rho_p c_p}{k}\frac{\partial \varphi}{\partial t}\sin(\gamma r)\, dr = \sqrt{\frac{2}{\pi}}\int_0^\infty \left[\frac{\partial^2 \varphi}{\partial r^2} + (\rho_b c_b \omega_b)\frac{\varphi}{k} + \frac{r}{k}(Q + P)\right]\sin(\gamma r)\, dr \qquad (10)$$

which implies,

$$K\frac{\partial \bar{\varphi}}{\partial t} = -(\omega^2 + \gamma^2)\bar{\varphi} + \frac{F(\gamma)}{k} \qquad (11)$$

where $K = \frac{\rho_p c_p}{k}$, $\omega^2 = \frac{\rho_b c_b \omega_b}{k}$, $\bar{\varphi} = \sqrt{\frac{2}{\pi}}\int_0^\infty \varphi \sin(\gamma r)\ dr$ and $F(\gamma) = \sqrt{\frac{2}{\pi}}\int_0^\infty rP(r)\sin(\gamma r)\, dr$

where γ is the Fourier transform variable and $\gamma \in (0, \infty)$. We omit the metabolic heat generation term $\frac{Q}{\rho_p c_p} \simeq 0$, (see Table 1).

Solution of equation (11) can be written as,

$$\bar{\varphi} = \exp[-(\omega^2 + \gamma^2)t]\bar{\varphi}_0 + \frac{F(\gamma)}{k(\omega^2+\gamma^2)}\left[1 - \exp\left(-\frac{(\omega^2+\gamma^2)t}{K}\right)\right] \qquad (12)$$

We assume that the initial temperature $T_0 = T_a$, the arterial blood temperature. Thus, we get $\bar{\varphi}_0 = 0$. Now applying the inverse Fourier transformation $\varphi = \sqrt{\frac{2}{\pi}}\int_0^\infty \bar{\varphi}(\gamma)\sin(\gamma r)\ d\gamma$, we obtain.

$$\varphi = \sqrt{\frac{2}{\pi}}\int_0^\infty \frac{F(\gamma)}{k(\omega^2+\gamma^2)}\left[1 - \exp\left(-\frac{(\omega^2+\gamma^2)t}{K}\right)\right]\sin(\gamma r)\, d\gamma \qquad (13)$$

Using $\frac{\varphi}{r} = \Phi$ and $\Phi - T_a = T$, we get the following equation.

$$T = T_a + \frac{1}{r}\sqrt{\frac{2}{\pi}}\int_0^\infty \frac{F(\gamma)}{k(\omega^2+\gamma^2)}\left[1 - \exp\left(-\frac{(\omega^2+\gamma^2)t}{K}\right)\right]\sin(\gamma r)\, d\gamma \qquad (14)$$

which gives the temperature profile inside the tumor mass at any time (t).

Since the heat source is a Gaussian distributed source: $P = P_0 \exp\left(-\frac{r^2}{r_0^2}\right)$, we have $F(\gamma) = \frac{1}{2\sqrt{2}} P_0 r_0^3 \gamma \exp\left(-\frac{\gamma^2 r_0^2}{4}\right)$, where r_0 is the extent of radial length up to which the magnetic fluid extends. The temperature inside the tumor mass at any time t can be obtained in two cases discussed below.

Case I: *Temperature For $0 < r < R$ at any time t.*

Using the above relation for $F(\gamma)$ in equation (14), we get the following equation:

$$T = T_a + \frac{P_0 r_0^3}{2\sqrt{\pi} k r} \int_0^\infty \frac{\gamma \exp\left(-\frac{\gamma^2 r_0^2}{4}\right)}{(\omega^2+\gamma^2)} \left[1 - \exp\left(-\frac{(\omega^2+\gamma^2)t}{K}\right)\right] \sin(\gamma r)\, d\gamma \quad (15)$$

which gives the temperature T at any time t and radius $0 < r < R$.

Case II: *Temperature for $r = 0$ at any time t.*

To obtain the temperature T at time t and $r = 0$, we substitute for $F(\gamma)$ and use L'Hospital's Rule and Leibniz Rule in succession in equation (14). Thus, at $r = 0$, we have

$$T = T_a + \frac{P_0 r_0^3}{2\sqrt{\pi} k} \int_0^\infty \frac{\gamma^2 \exp\left(-\frac{\gamma^2 r_0^2}{4}\right)}{(\omega^2+\gamma^2)} \left[1 - \exp\left(-\frac{(\omega^2+\gamma^2)t}{K}\right)\right] \sin(\gamma r)\, d\gamma \quad (16)$$

3.3. Steady state solution

Biological processes often undergo a transient phase before reaching a steady state. The steady state is a condition where the system's properties remain constant over time. This occurs when the system has settled into a stable equilibrium after the initial transient period. Mathematically, as time the transient effects diminish, and the system reaches its steady state. In this steady state, the solution to the governing equations no longer changes with time. This solution represents the long-term behavior of the system where all transient dynamics have dissipated.

The steady state solution to our model is obtained by letting $t \to \infty$ in equation (15) which is given by,

$$T = T_a + \frac{P_0 r_0^3}{2\sqrt{\pi} k r} \int_0^\infty \frac{\gamma \exp\left(-\frac{\gamma^2 r_0^2}{4}\right)}{(\omega^2+\gamma^2)} \sin(\gamma r)\, d\gamma \quad (17)$$

which gives the steady state temperature inside the tumor mass at time t and $0 < r < R$.

Steady state temperature at $r = 0$ is obtained by letting $t \to \infty$ in equation (16) which is given by,

$$T = T_a + \frac{P_0 r_0^3}{2\sqrt{\pi} k} \int_0^\infty \frac{\gamma^2 \exp\left(-\frac{\gamma^2 r_0^2}{4}\right)}{(\omega^2+\gamma^2)} \sin(\gamma r)\, d\gamma \quad (18)$$

Table 1. Numerical values of physiological parameters used in the model. [5, 12, 14, 17].

Quantity	Value
T_a	310 K
k	0.57 W $m^{-1} K^{-1}$
ρ_p	1079 Kg m^{-3}
ρ_b	1050 Kg m^{-3}
c_b	3600 J $kg^{-1} K^{-1}$
c_p	4180 J $kg^{-1} K^{-1}$
Q	7079.3 kg $m^{-3} s^{-1}$
w_b	6.4×10^{-3} s^{-1}
M_d	412 kA m^{-1}
K_U	9 kJ m^{-3}
D	10.9×10^{-9} m
ϕ	0.003

In this section, we illustrate the outcome of magnetic fluid hyperthermia using Gaussian source magnetite (Fe_3O_4) nanofluid on the primary hepatic tumor mass of size 2 cm inside a Chinese hamster. The values of various physiological parameters and other numerical values characteristic of the magnetic fluid are given in Table 1 below. The results are in close agreement with experimental research and existing literature [2, 3] further validating our model.

The radial temperature profile of the tumor mass at time (t) during magnetic fluid hyperthermia treatment under the Alternating Magnetic Field (AMF) and Rotating Magnetic Field (RMF) with $H_0 = 2.0kA$ and $f = 244\ kHz$ with $r_0 = 3$ mm and 5 mm are given in Fig. 4 and Fig. 5, respectively.

The graphs depict the temperature distribution along the radial distance of the tumor mass at different time intervals.

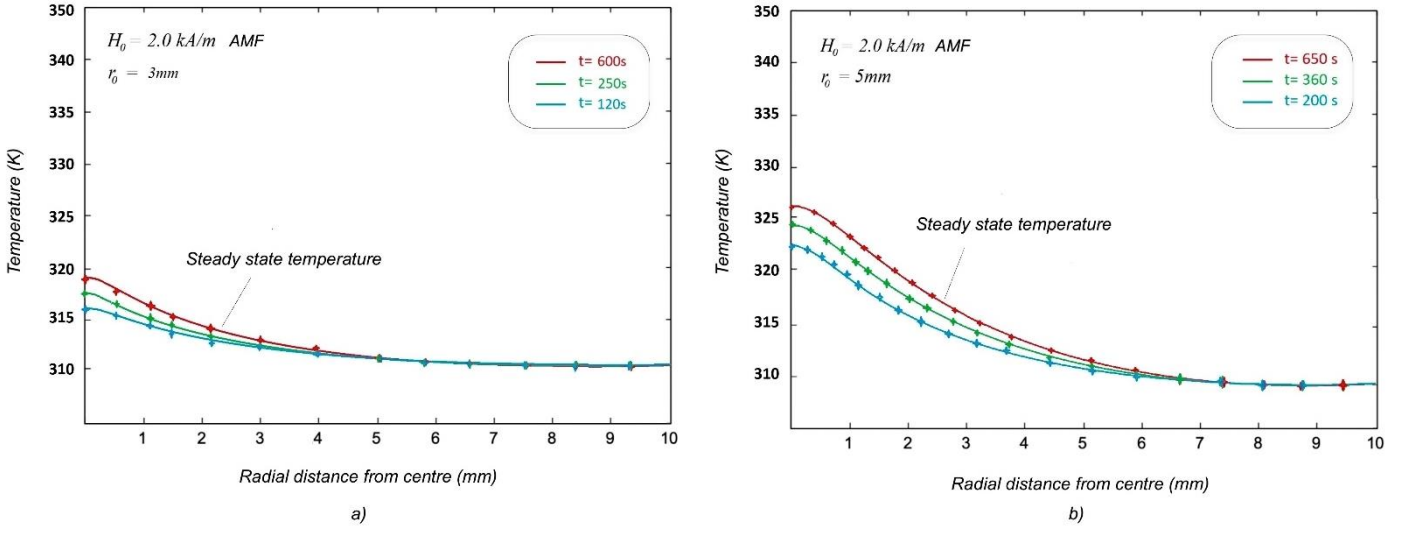

Fig. 4. Temperature profiles inside the tumor mass of size 2 cm during thermotherapy using magnetite (Fe_3O_4) nanoparticles under AMF with $H_0 = 2\ kA/m$ when the magnetic fluid extends to a radial length of; **a)** $r_0 = 3$ mm, and **b)** $r_0 = 5$ mm.

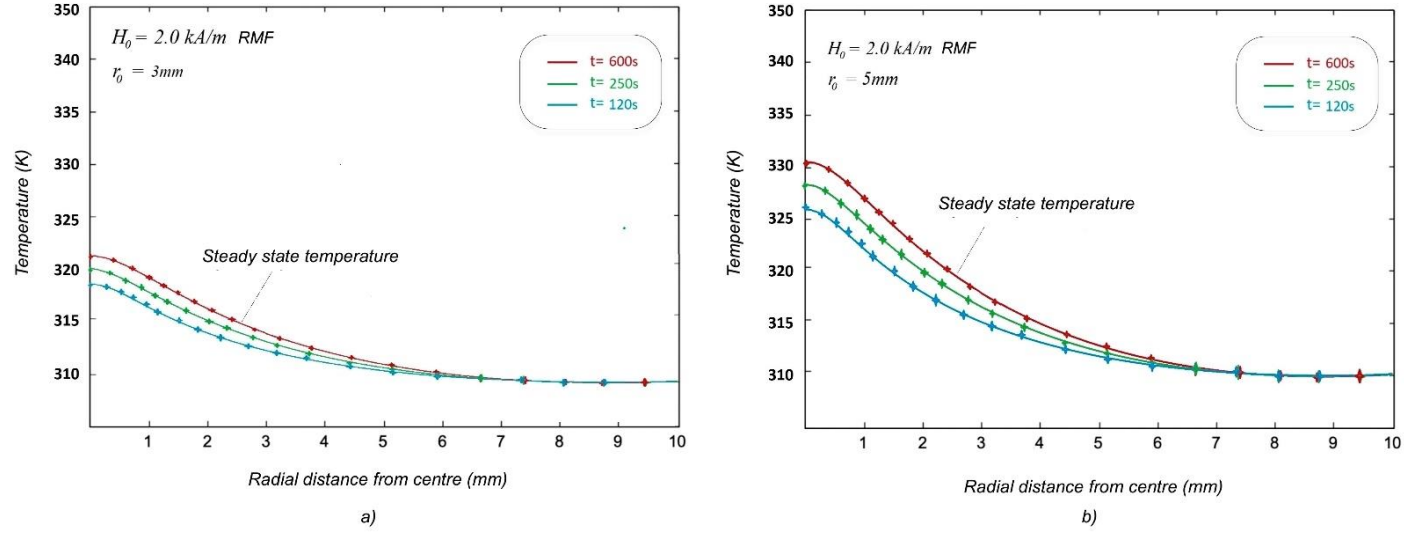

Fig. 5. Temperature profiles inside the tumor mass of size 2 cm during thermotherapy using magnetite (Fe_3O_4) nanoparticles under RMF when the magnetic fluid extends to a radial length of; **a)** $r_0 = 3$ mm, and **b)** $r_0 = 5$ mm.

Steady state temperatures (t_s), i.e., the maximum temperatures that are achieved subjected to the boundary conditions of equation (7) are also depicted in the graphs for the treatment under both the AMF and RMF.

The results depicted in Fig. 4 and Fig.5 show that the thermotherapy treatment using the given nanofluid is capable to raise the temperature of the tumor at the center to well above the threshold of 315 K (42°C). However, extent of the tumor mass affected by thermotherapy is increases with the increase in the volume covered by the injected nanofluid which is manifested by the value of r_0. The steady state temperature (T_s) obtained using 2.0 kA/m AMF for $r_0 = 3$ mm was 318 K at time $t_s = 600$ s, while the same for $r_0 = 5$ mm was 327 K at time $t_s = 650$ s. Similarly, in case of 2.0 kA/m RMF, for $r_0 = 3$ mm, a steady state temperature $T_s = 323$ K was obtained at time $t_s = 600$ s, and for for $r_0 = 5$ mm, $T_s = 332\ K$ was obtained at time $t_s = 600$ s.

4. CONCLUSION

Magnetic fluid hyperthermia (MFH) is an innovative, non-invasive treatment aimed at destroying tumors in difficult-to-reach or inoperable areas within the body. During hyperthermic treatment, it is crucial to maintain the

temperature of the surrounding healthy tissue below 315 K (42°C) to prevent cell damage. Typically, this requires the use of high sensitivity temperature sensors around the tumor, which makes the procedure invasive and unsuitable for certain inoperable areas. Our study overcomes this limitation by employing the well-established Pennes' Bio-Heat Equation validated with existing literature, to model heat transfer in biological tissues under appropriate boundary conditions. This method ensures that the temperature of healthy tissues surrounding the tumor remains within safe limits by applying magnetic fields only until the corresponding steady-state temperatures are reached. Thus, in practice, the optimal duration (t) for a single therapeutic session under a specific magnetic field strength should be shorter than the time (t_s) required to reach the steady-state temperature (T_s) as determined by the governing equation and boundary conditions. It is possible to extend the model for heterogeneous tumor mass by considering the thermal conductivity (k) as a function of tumor radial coordinate (r). Moreover, this study considers solid tumors only, thus limiting its applicability.

CONFLICT OF INTEREST

The authors declare that there is no conflict of interests.

REFERENCES

[1] Ahmed, A., Kim, E., Jeon, S., Kim, J.-Y. & Choi, H., **2022**. Closed-loop temperature controlled magnetic hyperthermia therapy with magnetic guidance of superparamagnetic iron-oxide nanoparticles *Advanced Therapeutics,* 5(2), p. 2100237.

[2] Beković, M., Trbušić, M., Trlep, M., Jesenik, M. and Hamler, A., **2018.** Magnetic Fluids' Heating Power Exposed to a High-Frequency Rotating Magnetic Field. *Advances in Materials Science and Engineering*, *2018*(1), p.6143607.

[3] Beković, M., Trlep, M., Jesenik, M. & Hamler, A., **2014**. A comparison of the heating effect of magnetic fluid between the alternating and rotating magnetic field. *Journal of Magnetism and Magnetic Materials,* 355, pp. 12–17.

[4] Chatterjee, D. K., Diagaradjane, P. & Krishnan, S., **2011**. Nanoparticle-mediated hyperthermia in cancer therapy. *Therapeutic Delivery,* 2(8), 1001–1014.

[5] Chen, C.-C. & Kiang, J.-F., **2018**. Efficacy of magnetic and capacitive hyperthermia on hepatocellular carcinoma. 2018 *IEEE International Symposium on Antennas and Propagation & USNC/URSI National Radio Science Meeting*. IEEE, pp. 385–386.

[6] Darvishi, V., Navidbakhsh, M. & Amanpour, S., **2022**. Heat and mass transfer in the hyperthermia cancer treatment by magnetic nanoparticles. *Heat and Mass Transfer,* 58(6), pp. 1029–1039.

[7] Deininger, P., **1999**. Genetic instability in cancer: caretaker and gatekeeper genes. *Ochsner Journal,* 1(4), pp. 206–209.

[8] Dieckhoff, J. H., Yoshida, T., Enpuku, K., Schilling, M. & Ludwig, F., **2012**. Homogeneous bioassays based on the manipulation of magnetic nanoparticles by rotating and alternating magnetic fields—a comparison. *IEEE Transactions on Magnetics,* 48(11), pp. 3792–3795.

[9] Galicia-Moreno, M., Silva-Gomez, J.A., Lucano-Landeros, S., Santos, A., Monroy-Ramirez, H.C. and Armendariz-Borunda, J., **2021.** Liver cancer: therapeutic challenges and the importance of experimental models. *Canadian Journal of Gastroenterology and Hepatology*, *2021*(1), p.8837811.

[10] Heinonen, I., Brothers, R. M., Kemppainen, J., Knuuti, J., Kalliokoski, K. K. & Crandall, C. G., 2011. Local heating, but not indirect whole-body heating, increases human skeletal muscle blood flow. *Journal of Applied Physiology,* 111(3), pp. 818–824.

[11] Ilg, P., Kröger, M., **2020**. Dynamics of interacting magnetic nanoparticles: Effective behavior from competition between Brownian and Néel relaxation. *Physical Chemistry Chemical Physics,* 22(39), pp. 22244–22259.

[12] Jordan, A., Scholz, R., Wust, P., Fähling, H., Krause, J., Wlodarczyk, W., Sander, B., Vogl, T. & Felix, R., **1997**. Effects of magnetic fluid hyperthermia (MFH) on c3h mammary carcinoma in vivo. *International Journal of Hyperthermia* 13(6), pp. 587–605.

[13] Lacis, S., **1999**. Bending of ferrofluid droplet in rotating magnetic field. *Journal of Magnetism and Magnetic Materials,* 201(1-3), pp. 335–338.

[14] Maenosono, S., Saita, S., **2006**. Theoretical assessment of FePt nanoparticles as heating elements for magnetic hyperthermia. *IEEE Transactions on Magnetics* 42(6), pp. 1638–1642.

[15] Mody, V. V., Singh, A. & Wesley, B., **2013**. Basics of magnetic nanoparticles for their application in the field of magnetic fluid hyperthermia. *European Journal of Nanomedicine* 5(1), pp. 11-21.

[16] Pennes, H. H., **1948**. Analysis of tissue and arterial

blood temperatures in the resting human forearm. *Journal of Applied Physiology,* 1(2), pp. 93–122.

[17] Radjenović, B., Sabo, M., Soltes, L., Prnova, M., Čičak, P. & Radmilović-Radjenović, M., **2021**. On efficacy of microwave ablation in the thermal treatment of an early-stage hepatocellular carcinoma. *Cancers* 13(22), p. 5784.

[18] Rosensweig, R. E., **2002**. Ferrofluids: magnetically controllable fluids and their applications. *Springer*, pp. 61–84.

[19] Van Cruchten, S. & Van Den Broeck, W., **2002**. Morphological and biochemical aspects of apoptosis, oncosis and necrosis. *Anatomia, Histologia, Embryologia,* 31(4), pp. 214–223.

[20] Wildeboer, R., Southern, P. & Pankhurst, Q., **2014**. On the reliable measurement of specific absorption rates and intrinsic loss parameters in magnetic hyperthermia materials. *Journal of Physics D: Applied Physics,* 47(49), p. 495003.

[21] Yoshida, T., Enpuku, K., Dieckhoff, J., Schilling, M. & Ludwig, F., **2012**. Magnetic fluid dynamics in a rotating magnetic field. *Journal of Applied Physics,* 111(5), p.053901.

[22] Zakinyan, A., Nechaeva, O. & Dikansky, Y., **2012**. Motion of a deformable drop of magnetic fluid on a solid surface in a rotating magnetic field. *Experimental Thermal and Fluid Science,* 39, pp. 265–268.